Exact Performance Analysis of AF Based Hybrid Satellite-Terrestrial Relay Network with Co-Channel Interference

Umer Javed[1], Di He[1], and Peilin Liu[1]
[1]Shanghai Key Laboratory of Navigation and Location-based Services, Shanghai Jiao Tong University, Shanghai 200240, China
[e-mail: umerjaved@sjtu.edu.cn, dihe@sjtu.edu.cn, liupeilin@sjtu.edu.cn]
Corresponding author*: Di He

Received January 5, 2015; revised March 26, 2014; revised May 25, 2015; revised June 28, 2015; accepted July 4, 2015; published September 30, 2015

Abstract

This paper considers the effect of co-channel interference on hybrid satellite-terrestrial relay network. In particular, we investigate the problem of amplify-and-forward (AF) relaying in hybrid satellite-terrestrial link, where the relay is interfered by multiple co-channel interferers. The direct link between satellite and terrestrial destination is not available due to masking by surroundings. The destination node can only receive signals from satellite with the assistance of a relay node situated at ground. The satellite-relay link is assumed to follow the shadowed Rice fading, while the channels of interferer-relay and relay-destination links experience Nakagami-*m* fading. For the considered AF relaying scheme, we first derive the analytical expression for the moment generating function (MGF) of the output signal-to-interference-plus-noise ratio (SINR). Then, we use the obtained MGF to derive the average symbol error rate (SER) of the considered scenario for M-ary phase shift keying (M-PSK) constellation under these generalized fading channels.

Keywords: Amplify-and-forward (AF) protocol, hybrid satellite-terrestrial relay network (HSTRN), co-channel interference (CCI), land mobile satellite (LMS) channel, M-ary phase-shift keying (M-PSK)

This research work is supported by the National High Technology Research and Development Program of China under Grant No. 2013AA013602, and the National Natural Science Foundation of China under Grant No. 91438113.

http://dx.doi.org/10.3837/tiis.2015.09.008 **ISSN : 1976-7277**

1. Introduction

Satellite systems are nowadays widely used in many diverse applications such as navigation, mobile communication, broadcasting, and disaster relief. So their proper functioning in many possible scenarios is very important from both users' and service providers' points of view. Due to increase in population density (especially in city centers), tall/wide buildings/structures and narrow streets/roads are very common at the present time. This results in for line-of-sight (LOS) communication difficult to be maintained because of shadowing and obstacles between satellite and terrestrial user [1]-[2]. This is also referred to as masking when LOS is lost between satellite and terrestrial user and it severely affects the indoor users being served by mobile satellite systems or in case of low satellite elevation angles.

A number of performance evaluations have been done by taking the above mentioned masking effect into consideration, especially for hybrid satellite-terrestrial cooperative networks (HSTCNs) [1]-[2]. Being one of the earliest performance analysis works, [3] gives the outage probability and the symbol error rate (SER) performance of HSTCN with multiple relays using a variable gain amplify-and-forward (AF) protocol. The average SER of the fixed gain AF HSTCN with generalized (Nakagami-*m*) fading channels has been derived in [4]. The channel between the satellite and terrestrial nodes (relay/destination) in [3] and [4] is assumed to follow the shadowed Rice land mobile satellite (LMS) model [5]. Different aspects of HSTCN have been studied in [6]-[9]. The outage performance of a HSTCN is analytically calculated in [10], where satellite links are assumed to suffer from shadowed Rice fading, while the terrestrial channel suffers from Nakagami-*m* fading. In [11], authors derive the exact outage probability of a HSTCN, where selective decode-and-forward (DF) protocol is implemented between the satellite and a terrestrial node, and a selection of the best relay terminal is performed. A slightly same system model of [11] is used in [12] to study the symbol error probability performance of a HSTCN, where in [12] no direct path from satellite to terrestrial (destination) node exists. In [13], authors investigate the performance of AF relaying in a hybrid satellite-terrestrial free space optical cooperative link with no direct connection between satellite and ground user. The use of multiple antennas (at relay & destination) in hybrid satellite-terrestrial cooperative system is considered in [14]. An approximate closed-form performance analysis of maximal ratio combining (MRC) in LMS channel of [5] is provided in [15]. The performance results of MRC over correlated $\kappa-\mu$ shadowed fading channels are obtained in [16].

All of the above mentioned papers have significantly increased our knowledge of performance analysis of HSTCN, however they have concentrated on ideal case without co-channel interference (CCI). The assumption of no CCI is unrealistic nowadays due to the deployment of many wireless standards, and increased practice of reusing the spectrum resource as much as possible in traditional wireless networks causes interference at relay/destination [17]-[20]. Different from the previous research, recently in [21] the effect of CCI on SER of HSTCN has been investigated. In [21], DF protocol is assumed at the terrestrial relay and the destination is corrupted by multiple CCI, both the satellite-destination and satellite-relay links undergo the shadowed Rice fading while the relay-destination link follows Rayleigh fading.

As we have mentioned above with the exception of [21], the effects of multiple CCI on the performance of dual-hop HSTCN have not been investigated in the open literature.

Specifically, we note that the performance analysis of three node AF based hybrid satellite-terrestrial relay network (HSTRN), with either single CCI or multiple CCI at the relay has not been done yet. As a result, in this paper, for hybrid satellite-terrestrial cooperative system, we analyze the average SER of M-PSK-modulated dual-hop fixed gain AF relay system with multiple interferers at the relay. We study a network with no direct connection between source (satellite) and destination (terrestrial mobile user), where a relay (terrestrial) forwards the source message to the destination. The direct link between satellite and destination is unavailable due to the following propagation impairments: the blocking of signals produced by large obstacles (shadowing), severe attenuation (path loss) and multipath fading. The above mentioned wireless propagation effects are most common in satellite to terrestrial radio links, that is why we study the relay network having no direct link from satellite to terrestrial receiver. We consider generalized fading channels where the source-relay (satellite-earth) link follows the shadowed Rice LMS model; and the relay-destination and interferers-relay links follow Nakagami-*m* fading. The system model proposed here is particularly applicable to frequency-division relay systems [22]-[23], where the relay and destination nodes experience different interference patterns. Also, the system model considered here is strongly motivated by the fact that multi-access relay techniques deal with many sources (satellites), which use the same relay in order to deliver their data to a single destination [24]. We derive the exact moment generating function (MGF) of the proposed network, based on the derived MGF the average SER of the considered relay network is obtained. Extensive performance analysis in the presence of multiple interferers for M-PSK modulation is done based on the expressions developed in the paper.

The remainder of this paper is organized as follows. Section 2 gives the detailed system model of considered dual-hop relay network. Section 3 details the performance analysis of the proposed system model. Specifically, MGF of the cooperative link is derived and, based on this exact MGF analytical expression for SER of the cooperative link is given. Section 4 presents the detailed numerical results. Finally, Section 5 concludes this paper.

2. System Model

We consider a hybrid/integrated satellite-terrestrial communication system, where a satellite communicates with a destination node at ground through a relay node located at ground. It is assumed that satellite does not have a direct link to destination node. The communication in the system is divided into two orthogonal phases. In the first phase, the satellite sends its signal to the relay. At relay, the received signal in the presence of n interferers, will be

$$y_1 = h_1 x + \left(\sum_{j=1}^{n} h_{3j} y_j \right) + n_1, \tag{1}$$

where h_1 is the channel gain between the satellite and the relay; x is the satellite's transmitted symbol with E_s power; h_{3j} is the channel gain between the jth interferer and the relay; y_j is the jth interferer's transmitted symbol with E_{ij} power; n_1 is the zero-mean additive white Gaussian noise (AWGN) at relay with σ_1^2 variance.

In the second phase, the relay multiplies the received signal y_1 with a fixed gain $G > 0$. The amplified signal is forwarded (sent) to the destination. The received signal at destination is given by

$$y_2 = Gh_2\left(h_1 x + \left(\sum_{j=1}^{n} h_{3j} y_j\right) + n_1\right) + n_2, \tag{2}$$

where h_2 is the channel gain between the relay and the destination, and n_2 is AWGN at destination with σ_2^2 variance.

The satellite-relay link is assumed to follow the shadowed Rice fading channel with the following probability density function (PDF) [4]-[5]

$$f_{|h_1|^2}(x) = \alpha_1 e^{-\beta_1 x} {}_1F_1(m_1;1;\delta_1 x), x \geq 0, \tag{3}$$

where $\alpha_1 = \frac{1}{2b_1}\left(\frac{2b_1 m_1}{2b_1 m_1 + \Omega_1}\right)^{m_1}$, $\beta_1 = \frac{1}{2b_1}$, $\delta_1 = \frac{\Omega_1}{2b_1(2b_1 m_1 + \Omega_1)}$, Ω_1 is the average power of LOS component, $2b_1$ is the average power of the multipath component, ${}_1F_1(a;b;z)$ is the confluent hypergeometric function [25, Eq. (9.210.1)], and $0 \leq m_1 \leq \infty$ is the Nakagami parameter. For $m_1 = 0$, (3) simplifies to the Rayleigh PDF in (4), while for $m_1 = \infty$, it reduces to the Rice PDF. In the shadowed Rice model of [5], the scattered component of the received signal follows Rayleigh distribution and LOS component follows a Nakagami-*m* distribution as follows:

$$p_X(x) = \frac{x}{b_0}\exp\left(\frac{-x^2}{2b_0}\right), \tag{4}$$

$$p_Y(y) = \frac{2m^m}{\Gamma(m)\Omega^m} y^{2m-1}\exp\left(\frac{-my^2}{\Omega}\right), \tag{5}$$

where $2b_0 = E\left[X^2\right]$ is the average power of the scatter (multipath) component, $\Gamma(.)$ is the gamma function, $m = \frac{\left(E\left[Y^2\right]\right)^2}{Var\left[Y^2\right]} \geq 0$ is the Nakagami parameter, and $\Omega = E\left[Y^2\right]$ is the average power of the LOS component.

The relay-destination link is assumed to follow the Nakagami-*m* distribution; hence, $|h_2|^2$ follows the Gamma distribution [4] as

$$f_{|h_2|^2}(x) = \lambda_2 x^{m_2 - 1} e^{-\varepsilon_2 x}, x \geq 0, \tag{6}$$

where $\lambda_2 = \frac{(m_2/\Omega_2)^{m_2}}{\Gamma(m_2)}$, $\varepsilon_2 = \frac{m_2}{\Omega_2}$; and $\frac{1}{2} \leq m_2 \leq \infty$ and Ω_2 denote the shape and scale parameters, respectively, of the relay-destination channel.

The interferer-relay link is assumed to follow the Nakagami-*m* distribution; hence, $\left|h_{3j}\right|^2$ follows the Gamma distribution [4] as

$$f_{|h_{3j}|^2}(x) = \lambda_{3j} x^{m_{3j} - 1} e^{-\varepsilon_{3j} x}, x \geq 0, \tag{7}$$

where $\lambda_{3j} = \frac{\left(m_{3j}/\Omega_{3j}\right)^{m_{3j}}}{\Gamma\left(m_{3j}\right)}$, $\varepsilon_{3j} = \frac{m_{3j}}{\Omega_{3j}}$; and $\frac{1}{2} \leq m_{3j} \leq \infty$ and Ω_{3j} denote the shape and scale parameters, respectively, of the interferer-relay channel.

3. Performance Analysis

In this section, we will derive the average SER of the system model described in Section 2. We follow the standard MGF based approach [26]. The overall signal-to-interference-plus-noise ratio (SINR) γ can be written [27]-[28], by using (2), as

$$\gamma = \frac{E_s |h_1|^2 |h_2|^2}{|h_2|^2 \sigma_1^2 + |h_2|^2 \left(\sum_{j=1}^{n} E_{ij} |h_{3j}|^2 \right) + \frac{\sigma_2^2}{G^2}} \stackrel{(a)}{=} \frac{E_s |h_1|^2 |h_2|^2}{|h_2|^2 \sigma_1^2 + E_i |h_2|^2 |h_3|^2 + \frac{\sigma_2^2}{G^2}}. \tag{8}$$

In case of equal-power interferers ($E_{ij} = E_i$, for $j = 1,2,...n$), the step (a) in (8) follows from the use of the following property (summation) of Gamma distribution. When $|h_{3j}|^2$ has a Gamma (m_{3j}, Ω_3) distribution for $j = 1,2,...,n$ (i.e., all distributions have the same scale parameter Ω_3), then,

$$\sum_{j=1}^{n} |h_{3j}|^2 \sim Gamma\left(\sum_{j=1}^{n} m_{3j}, \Omega_3 \right),$$

provided that all $|h_{3j}|^2$ are independent. In case of arbitrarily powered (unequal-power) interferers $E_{i1} \neq E_{i2} \neq, ..., \neq E_{in}$, the step (a) in (8) follows by first applying the scaling property of the Gamma distribution, and then using the summation property of Gamma distribution. The scaling property says that, when $|h_{3j}|^2 \sim Gamma(m_{3j}, \Omega_{3j})$ for $j = 1,2,...,n$, then for any $E_{ij} > 0$, $E_{ij} |h_{3j}|^2 \sim Gamma(m_{3j}, E_{ij}\Omega_{3j})$. Here, for the sake of mathematical tractability and analytical simplicity we assume that $E_{i1}\Omega_{31} = E_{i2}\Omega_{32} =, ..., E_{in}\Omega_{3n}$, so that after scaling and summation operations, respectively, the result of the sum $\left(\sum_{j=1}^{n} E_{ij} |h_{3j}|^2 \right)$, denoted by $E_i |h_3|^2$, still follows the Gamma distribution.

Alternatively, (8) can also be written as

$$\gamma = \frac{|h_1|^2 |h_2|^2}{|h_2|^2 + \frac{E_i}{\sigma_1^2} |h_2|^2 |h_3|^2 + \frac{\sigma_2^2}{\sigma_1^2 G^2}} \frac{E_s}{\sigma_1^2}. \tag{9}$$

On substituting $C = \frac{\sigma_2^2}{\sigma_1^2 G^2}$ in (9), we finally get

$$\gamma = \frac{|h_1|^2 |h_2|^2}{|h_2|^2 + \frac{E_i}{\sigma_1^2} |h_2|^2 |h_3|^2 + C} \frac{E_s}{\sigma_1^2} = \frac{|h_1|^2 |h_2|^2}{|h_2|^2 + \overline{\gamma}_{\text{int}} |h_2|^2 |h_3|^2 + C} \overline{\gamma}, \tag{10}$$

where in (10), $\overline{\gamma} = \overline{\gamma_1} = \frac{E_s}{\sigma_1^2}$ is the average signal-to-noise-ratio (SNR), and $\overline{\gamma_{\text{int}}} = \overline{\gamma_3} = \frac{E_i}{\sigma_1^2}$ is the equivalent interference-to-noise-ratio (INR) of interferer-relay links.

3.1 Calculation of the MGF of the Considered System Model

The MGF of the considered system model can be written as

$$M_\gamma(s) = E_\gamma\left[e^{-s\frac{|h_1|^2|h_2|^2}{|h_2|^2 + \frac{E_i}{\sigma_1^2}|h_2|^2|h_3|^2 + C}\frac{E_s}{\sigma_1^2}} \right]$$

$$= \int_0^\infty\int_0^\infty\int_0^\infty e^{\left(-s\frac{xy}{y\left(1+z\frac{E_i}{\sigma_1^2}\right)+C}\frac{E_s}{\sigma_1^2}\right)} f_{|h_1|^2}(x) f_{|h_2|^2}(y)\, f_{|h_3|^2}(z)\,dxdydz. \tag{11}$$

We pick and define the following integral from the above triple-integral:

$$I_1 \triangleq \int_0^\infty e^{\left(-s\frac{xy}{y\left(1+z\frac{E_i}{\sigma_1^2}\right)+C}\frac{E_s}{\sigma_1^2}\right)} f_{|h_1|^2}(x)\,dx. \tag{12}$$

It can be proved in Appendix I that

$$I_1 = \frac{\left(\alpha_1\left(1+z\frac{E_i}{\sigma_1^2}\right)y+\alpha_1 C\right)\left(\left(s\frac{E_s}{\sigma_1^2}+\beta_1\left(1+z\frac{E_i}{\sigma_1^2}\right)\right)y+C\beta_1\right)^{m_1-1}}{\left(\left(s\frac{E_s}{\sigma_1^2}+(\beta_1-\delta_1)\left(1+z\frac{E_i}{\sigma_1^2}\right)\right)y+C(\beta_1-\delta_1)\right)^{m_1}}. \tag{13}$$

Let us now define the following integral from (11) by using I_1 :

$$I_2 \triangleq \int_0^\infty I_1 f_{|h_2|^2}(y)\,dy. \tag{14}$$

We substitute (13) and (6) in (14), and get the following

$$I_2 = \int_0^\infty \frac{\left(\alpha_1\left(1+z\frac{E_i}{\sigma_1^2}\right)y+\alpha_1 C\right)\left(\left(s\frac{E_s}{\sigma_1^2}+\beta_1\left(1+z\frac{E_i}{\sigma_1^2}\right)\right)y+C\beta_1\right)^{m_1-1}}{\left(\left(s\frac{E_s}{\sigma_1^2}+(\beta_1-\delta_1)\left(1+z\frac{E_i}{\sigma_1^2}\right)\right)y+C(\beta_1-\delta_1)\right)^{m_1}} \lambda_2 y^{m_2-1} e^{-\varepsilon_2 y}\,dy. \tag{15}$$

By using the method outlined in [4], (15) becomes

$$I_2=\lambda_2\int_0^\infty \frac{\left(\alpha_1\left(1+z\frac{E_i}{\sigma_1^2}\right)y+\alpha_1 C\right)\left(\left(s\frac{E_s}{\sigma_1^2}+\beta_1\left(1+z\frac{E_i}{\sigma_1^2}\right)\right)y+C\beta_1\right)^{c_1}}{\left(\left(s\frac{E_s}{\sigma_1^2}+(\beta_1-\delta_1)\left(1+z\frac{E_i}{\sigma_1^2}\right)\right)y+C(\beta_1-\delta_1)\right)^{m_1}}$$
$$\times\left(\left(s\frac{E_s}{\sigma_1^2}+\beta_1\left(1+z\frac{E_i}{\sigma_1^2}\right)\right)y+C\beta_1\right)^{e} y^{m_2-1}e^{-\varepsilon_2 y}dy, \tag{16}$$

where $c_1=\lfloor m_1\rfloor-1$ and $e=m_1-\lfloor m_1\rfloor$ for $m_1>1$; $c_1=0$ and $e=m_1-1$ for $m_1\le 1$;and $\lfloor x\rfloor$ denotes the largest integer not greater than x . By the use of Binomial expansion

$$(x+y)^n=\sum_{m=0}^{n}\left(\frac{n!}{m!(n-m)!}\right)x^{n-m}y^m,\ x,y\in R,\ n\in Z^+,$$

in (16), we rewrite (16) as

$$I_2=\lambda_2\sum_{l=0}^{c_1}\binom{c_1}{l}\left(s\frac{E_s}{\sigma_1^2}+\beta_1\left(1+z\frac{E_i}{\sigma_1^2}\right)\right)^{l}(C\beta_1)^{c_1-l}$$
$$\times\int_0^\infty \frac{\left(\alpha_1\left(1+z\frac{E_i}{\sigma_1^2}\right)y+\alpha_1 C\right)\left(\left(s\frac{E_s}{\sigma_1^2}+\beta_1\left(1+z\frac{E_i}{\sigma_1^2}\right)\right)y+C\beta_1\right)^{e} y^{m_2+l-1}e^{-\varepsilon_2 y}}{\left(\left(s\frac{E_s}{\sigma_1^2}+(\beta_1-\delta_1)\left(1+z\frac{E_i}{\sigma_1^2}\right)\right)y+C(\beta_1-\delta_1)\right)^{m_1}}dy. \tag{17}$$

Now we employ the following approximation $(1+x)^\eta\approx 1+\eta x, x<1$ in (17), and after applying some elementary algebraic operations (for details see Appendix II), we obtain

$$I_2\cong P_1-P_2+P_3, \tag{18}$$

where,

$$P_1=\sum_{l=0}^{c_1}\binom{c_1}{l}\frac{\lambda_2(C\beta_1)^{m_1+m_2-1}}{\left(s\frac{E_s}{\sigma_1^2}+\beta_1\left(1+z\frac{E_i}{\sigma_1^2}\right)\right)^{m_2}}\int_0^1 e^{\frac{-\varepsilon_2 C\beta_1 x}{s\frac{E_s}{\sigma_1^2}+\beta_1\left(1+z\frac{E_i}{\sigma_1^2}\right)}}\left(\frac{\left(1+z\frac{E_i}{\sigma_1^2}\right)\alpha_1 C\beta_1 x}{s\frac{E_s}{\sigma_1^2}+\beta_1\left(1+z\frac{E_i}{\sigma_1^2}\right)}+\alpha_1 C\right)$$
$$\times\left(\frac{\left(s\frac{E_s}{\sigma_1^2}+(\beta_1-\delta_1)\left(1+z\frac{E_i}{\sigma_1^2}\right)\right)C\beta_1 x}{s\frac{E_s}{\sigma_1^2}+\beta_1\left(1+z\frac{E_i}{\sigma_1^2}\right)}+C(\beta_1-\delta_1)\right)^{-m_1} x^{m_2+l-1}(1+ex)dx, \tag{19}$$

$$P_2=\sum_{l=0}^{c_1}\binom{c_1}{l}\frac{\lambda_2\left(C\beta_1\right)^{m_1+m_2-1}}{\left(s\frac{E_s}{\sigma_1^2}+\beta_1\left(1+z\frac{E_i}{\sigma_1^2}\right)\right)^{m_2}}\int_0^1 e^{\frac{-\varepsilon_2 C\beta_1 x}{s\frac{E_s}{\sigma_1^2}+\beta_1\left(1+z\frac{E_i}{\sigma_1^2}\right)}}\left(\frac{\left(1+z\frac{E_i}{\sigma_1^2}\right)\alpha_1 C\beta_1 x}{s\frac{E_s}{\sigma_1^2}+\beta_1\left(1+z\frac{E_i}{\sigma_1^2}\right)}+\alpha_1 C\right)$$
$$\times\left(\frac{\left(s\frac{E_s}{\sigma_1^2}+\left(\beta_1-\delta_1\right)\left(1+z\frac{E_i}{\sigma_1^2}\right)\right)C\beta_1 x}{s\frac{E_s}{\sigma_1^2}+\beta_1\left(1+z\frac{E_i}{\sigma_1^2}\right)}+C\left(\beta_1-\delta_1\right)\right)^{-m_1} x^{e+m_2+l-1}\left(1+\frac{e}{x}\right)dx, \tag{20}$$

$$P_3=\lambda_2\sum_{l=0}^{c_1}\binom{c_1}{l}\left(s\frac{E_s}{\sigma_1^2}+\beta_1\left(1+z\frac{E_i}{\sigma_1^2}\right)\right)^{l+e}\left(C\beta_1\right)^{c_1-l}\left\{\frac{\alpha_1 C^2\beta_1 e}{s\frac{E_s}{\sigma_1^2}+\beta_1\left(1+z\frac{E_i}{\sigma_1^2}\right)}f\left(e+m_2+l-2\right)\right.$$
$$\left.+\alpha_1 C\left(1+\frac{\left(1+z\frac{E_i}{\sigma_1^2}\right)\beta_1 e}{s\frac{E_s}{\sigma_1^2}+\beta_1\left(1+z\frac{E_i}{\sigma_1^2}\right)}\right)f\left(e+m_2+l-1\right)+\alpha_1 f\left(e+m_2+l\right)\right\}. \tag{21}$$

The MGF of the considered system model can now be written, using (11) and I_2, as

$$M_\gamma\left(s\right)=\int_0^\infty I_2 f_{|h_3|^2}\left(z\right)dz$$
$$=\int_0^\infty I_2\lambda_3 z^{m_3-1}e^{-\varepsilon_3 z}dz. \tag{22}$$

By putting (18) in (22), and after rearrangement of integrals and sums, we write the expression for MGF of our proposed system as

$$M_\gamma\left(s\right)=M_1-M_2+M_3+M_4+M_5. \tag{23}$$

In (23)

$$M_1=\lambda_2\lambda_3\left(C\beta_1\right)^{m_1+m_2-1}\sum_{l=0}^{c_1}\binom{c_1}{l}\left\{\int_0^1 x^{m_2+l-1}\left(1+ex\right)e^{\frac{-\varepsilon_2 C\beta_1 x}{s\frac{E_s}{\sigma_1^2}+\beta_1\left(1+z\frac{E_i}{\sigma_1^2}\right)}}\left(\frac{\left(1+z\frac{E_i}{\sigma_1^2}\right)\alpha_1 C\beta_1 x}{s\frac{E_s}{\sigma_1^2}+\beta_1\left(1+z\frac{E_i}{\sigma_1^2}\right)}+\alpha_1 C\right)\right.$$
$$\left.\times\left(\frac{\left(s\frac{E_s}{\sigma_1^2}+\left(\beta_1-\delta_1\right)\left(1+z\frac{E_i}{\sigma_1^2}\right)\right)C\beta_1 x}{s\frac{E_s}{\sigma_1^2}+\beta_1\left(1+z\frac{E_i}{\sigma_1^2}\right)}+C\left(\beta_1-\delta_1\right)\right)^{-m_1}dx\int_0^\infty\frac{z^{m_3-1}e^{-\varepsilon_3 z}}{\left(s\frac{E_s}{\sigma_1^2}+\beta_1\left(1+z\frac{E_i}{\sigma_1^2}\right)\right)^{m_2}}dz\right\}, \tag{24}$$

$$M_2 = \lambda_2\lambda_3\left(C\beta_1\right)^{m_1+m_2-1}\sum_{l=0}^{c_1}\binom{c_1}{l}\left\{\int_0^1 x^{e+m_2+l-1}\left(1+\frac{e}{x}\right)e^{\frac{-\varepsilon_2 C\beta_1 x}{s\frac{E_s}{\sigma_1^2}+\beta_1\left(1+z\frac{E_i}{\sigma_1^2}\right)}}\right.$$

$$\times\left(\frac{\left(1+z\frac{E_i}{\sigma_1^2}\right)\alpha_1 C\beta_1 x}{s\frac{E_s}{\sigma_1^2}+\beta_1\left(1+z\frac{E_i}{\sigma_1^2}\right)}+\alpha_1 C\right)\left(\frac{\left(s\frac{E_s}{\sigma_1^2}+\left(\beta_1-\delta_1\right)\left(1+z\frac{E_i}{\sigma_1^2}\right)\right)C\beta_1 x}{s\frac{E_s}{\sigma_1^2}+\beta_1\left(1+z\frac{E_i}{\sigma_1^2}\right)}+C\left(\beta_1-\delta_1\right)\right)^{-m_1} dx$$

$$\left.\times\int_0^\infty\frac{z^{m_3-1}e^{-\varepsilon_3 z}}{\left(s\frac{E_s}{\sigma_1^2}+\beta_1\left(1+z\frac{E_i}{\sigma_1^2}\right)\right)^{m_2}}dz\right\}, \tag{25}$$

$$M_3 = \alpha_1\lambda_2\lambda_3 C^{1+c_1+e+m_2-m_1}\sum_{l=0}^{c_1}\binom{c_1}{l}\beta_1^{c_1-l}\left(\beta_1-\delta_1\right)^{e+l+m_2-m_1}$$

$$\times\left\{\int_0^\infty e^{-\frac{\varepsilon_2 C\left(\beta_1-\delta_1\right)}{s\frac{E_s}{\sigma_1^2}+\left(\beta_1-\delta_1\right)\left(1+z\frac{E_i}{\sigma_1^2}\right)}t} t^{e+l+m_2-1}\left(1+t\right)^{-m_1} dt\right.$$

$$\left.\times\int_0^\infty\left(1+\frac{\left(1+z\frac{E_i}{\sigma_1^2}\right)e\beta_1}{s\frac{E_s}{\sigma_1^2}+\beta_1\left(1+z\frac{E_i}{\sigma_1^2}\right)}\right)\frac{\left(s\frac{E_s}{\sigma_1^2}+\beta_1\left(1+z\frac{E_i}{\sigma_1^2}\right)\right)^{e+l}}{\left(s\frac{E_s}{\sigma_1^2}+\left(\beta_1-\delta_1\right)\left(1+z\frac{E_i}{\sigma_1^2}\right)\right)^{e+l+m_2}}z^{m_3-1}e^{-\varepsilon_3 z}dz\right\}, \tag{26}$$

$$M_4 = \alpha_1\lambda_2\lambda_3 C^{1+c_1+e+m_2-m_1}\sum_{l=0}^{c_1}\binom{c_1}{l}\beta_1^{c_1-l}\left(\beta_1-\delta_1\right)^{e+l+m_2-m_1+1}$$

$$\times\left\{\int_0^\infty e^{-\frac{\varepsilon_2 C\left(\beta_1-\delta_1\right)}{s\frac{E_s}{\sigma_1^2}+\left(\beta_1-\delta_1\right)\left(1+z\frac{E_i}{\sigma_1^2}\right)}t} t^{e+l+m_2}\left(1+t\right)^{-m_1} dt\right.$$

$$\left.\times\int_0^\infty\left(1+z\frac{E_i}{\sigma_1^2}\right)\frac{\left(s\frac{E_s}{\sigma_1^2}+\beta_1\left(1+z\frac{E_i}{\sigma_1^2}\right)\right)^{e+l}}{\left(s\frac{E_s}{\sigma_1^2}+\left(\beta_1-\delta_1\right)\left(1+z\frac{E_i}{\sigma_1^2}\right)\right)^{(e+l+m_2+1)}}z^{m_3-1}e^{-\varepsilon_3 z}dz\right\}, \tag{27}$$

$$M_5 = \alpha_1 \lambda_2 \lambda_3 C^{1+c_1+e+m_2-m_1} \sum_{l=0}^{c_1} \binom{c_1}{l} \beta_1^{c_1-l+1} \left(\beta_1-\delta_1\right)^{e+l+m_2-m_1-1}$$
$$\times \left\{ \int_0^\infty e^{-\frac{\varepsilon_2 C(\beta_1-\delta_1)}{s\frac{E_s}{\sigma_1^2}+(\beta_1-\delta_1)\left(1+z\frac{E_i}{\sigma_1^2}\right)}t} t^{e+l+m_2-2} \left(1+t\right)^{-m_1} dt \right.$$
$$\left. \times \int_0^\infty \left(s\frac{E_s}{\sigma_1^2} + \beta_1 \left(1+z\frac{E_i}{\sigma_1^2}\right)\right)^{e+l-1} \left(s\frac{E_s}{\sigma_1^2} + \left(\beta_1-\delta_1\right)\left(1+z\frac{E_i}{\sigma_1^2}\right)\right)^{-(e+l+m_2-1)} z^{m_3-1} e^{-\varepsilon_3 z} dz \right\}. \quad (28)$$

It can be seen from (24)-(28) that MGF contains finite and infinite integrals, which can be accurately/easily calculated in MATLAB or Mathematica.

3.2 Calculation of SER

The SER of the considered HSTCN for M-PSK constellation is given by [4], [26] as:

$$P_{MPSK} = \frac{1}{\pi} \int_0^{\theta_M} M_\gamma \left(\frac{g_{MPSK}}{\sin^2 \theta} \right) d\theta, \quad (29)$$

where $\theta_M = \frac{\pi(M-1)}{M}$ and $g_{MPSK} = \sin^2\left(\frac{\pi}{M}\right)$.

Alternatively, the following accurate approximation of (29) can be used from [29]:

$$P_{MPSK} = \sum_{p=1}^{3} b_p M_\gamma \left(a_p\right), \quad (30)$$

where $b_1 = \frac{\theta_M}{2\pi} - \frac{1}{6}, b_2 = \frac{1}{4}, b_3 = \frac{\theta_M}{2\pi} - \frac{1}{4}, a_1 = g_{MPSK}, a_2 = 4\frac{g_{MPSK}}{3}$ and $a_3 = \frac{g_{MPSK}}{\sin^2\left(\theta_M\right)}$.

4. Numerical Results

This section presents the analytical and simulated results of the considered AF based HSTRN scheme using M-PSK modulation over generalized fading channels. We demonstrate the expressions derived in Section 3 using numerical examples and study the effect of interference on the system's performance. The simulated results are obtained by generating 10^7 channel realizations for BPSK, QPSK and 8-PSK symbols. It is assumed that relay-destination channel & interference channels follow the Nakagami-*m* fading with parameters taken from [22]. The satellite-relay LMS channel is varied according to different shadowing conditions. The parameters of the shadowed Rice LMS model are shown in **Table 1**.

Table 1. LMS channel parameters [5]

Shadowing	b_i	m_i	Ω_i
Frequent heavy shadowing	0.063	0.739	8.97×10^{-4}
Average shadowing	0.126	10.1	0.835
Infrequent light shadowing	0.158	19.4	1.29

Fig. 1 shows the average SER versus SNR of the considered HSTRN, for infrequent light shadowing (satellite-relay LMS channel), with multiple values of CCI (-5 dB, 0 dB and 5dB) using different M-PSK modulation schemes: BPSK, QPSK and 8-PSK. It is assumed that $\sigma_1^2 = \sigma_2^2$; and on the x-axis of **Fig. 1 (a)**, **Fig. 1 (b)** & **Fig. 1 (c)**, SNR denotes $\overline{\gamma}$; CCI represents $\overline{\gamma}_{\text{int}}$. We consider the situation when relay is interfered by three equal-power interferers, i.e., $n = 3$, and $\overline{\gamma}_{\text{int},i} = \overline{\gamma}_{int}/n$ is the CCI caused by each interferer $i \le n$. The values of total CCI $\overline{\gamma}_{\text{int}}$ experienced by the source to relay link are selected as: -5 dB, 0 dB and 5dB. Any other appropriate value of CCI could be used by system designer based on specific conditions. Note that our considered system model and analysis deals with the case of arbitrary number of interferers having different transmit powers and channel parameters (already described in Section 3). Here, for simplicity and illustration purposes we consider a most common subset of this case, i.e., multiple equal-power independent interferers. The theoretical SER is plotted by using (30). **Fig. 2** presents the average SER versus SNR of the considered HSTRN, for average shadowing (satellite-relay LMS channel), with multiple values of CCI (-5 dB, 0 dB and 5dB) using different M-PSK modulation schemes: BPSK, QPSK and 8-PSK. **Fig. 3** illustrates the average SER versus SNR of the considered HSTRN, for frequent heavy shadowing (satellite-relay LMS channel), with multiple values of CCI (-5 dB, 0 dB and 5dB) using different M-PSK modulation schemes: BPSK, QPSK and 8-PSK. The above discussion about values of network parameters for **Fig. 1** is also valid for **Fig. 2** & **Fig. 3**. We observe from **Fig. 1**, **Fig. 2** & **Fig. 3** that simulated SER very closely follows the analytical SER, for all shadowing situations and modulations, considered in the figures; indicating the correctness of the approximations taken and derived analytical formula.

As we can see from **Fig. 1**, **Fig. 2** & **Fig. 3**, that when CCI at relay increases from -5 dB to +5 dB, there is a notable increase in average SER of the considered system for a given modulation format. We observe that the increase in SER is more prominent for higher-order modulation such as 8-PSK than that of lower-order modulation scheme of BPSK. This can be seen from **Fig. 1**, **Fig. 2** and **Fig. 3**, e.g., by comparing the curves for 8-PSK and BPSK for the same value of given CCI. The same reasoning is also valid for comparing combinations of 8-PSK/QPSK and QPSK/BPSK. When LMS channel experiences increase in amount of shadowing, as shown by the sequence of **Fig. 1**, **Fig. 2** and **Fig. 3**, respectively, we notice that the average SER of the HSTRN also increases correspondingly. The reader can view the effect of shadowing on the considered system by comparing the curves for particular modulation with the same given CCI from **Fig. 1**, **Fig. 2** and **Fig. 3**. We also comment here about the computational time of the expression for MFG in (23) since it contains multiple integrals. We tested in MATLAB that for different SNRs (dB), e.g. {10, 20, 30}, modern personal computer takes approximately 0.2 seconds to calculate (23). The impact of the fading severity of the relay-destination link, namely nakagami m_2 parameter, is shown in **Fig. 4**. The analysis is done for QPSK modulated HSTRN with 0 dB CCI over average shadowed LMS source-relay channel. It can be observed from **Fig. 4** that, with the increase in value of m_2 (decrease in amount or degree of fading), there is a corresponding decrease in SER. The impact of the fading severity of the interferers-relay links, namely nakagami m_3 parameter, is shown in **Fig. 5**. The study is done for QPSK modulated HSTRN with multiple values of m_3 amounting to different CCIs over average shadowed LMS source-relay channel. It can be observed from **Fig. 5** that, with the increase in value of m_3 (decrease in amount or degree of fading), there is a corresponding increase in SER. The increase in SER is due to the fact that with decrease in amount or degree of fading, the power of the interferers' signal increases and so do the resulting CCI caused by it.

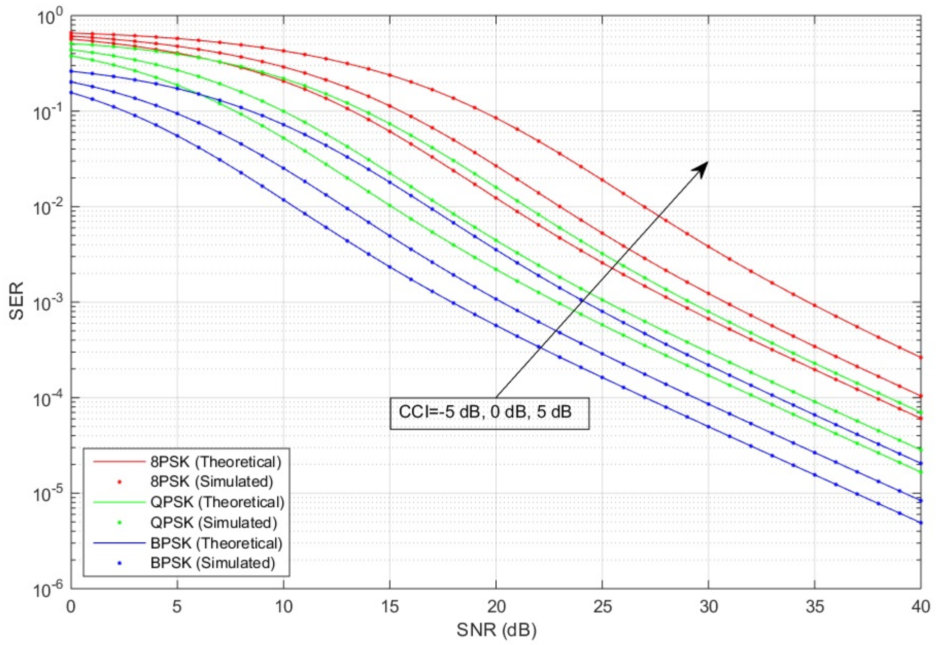

Fig. 1. Average SER versus SNR for M-PSK with CCI in infrequent light shadowing

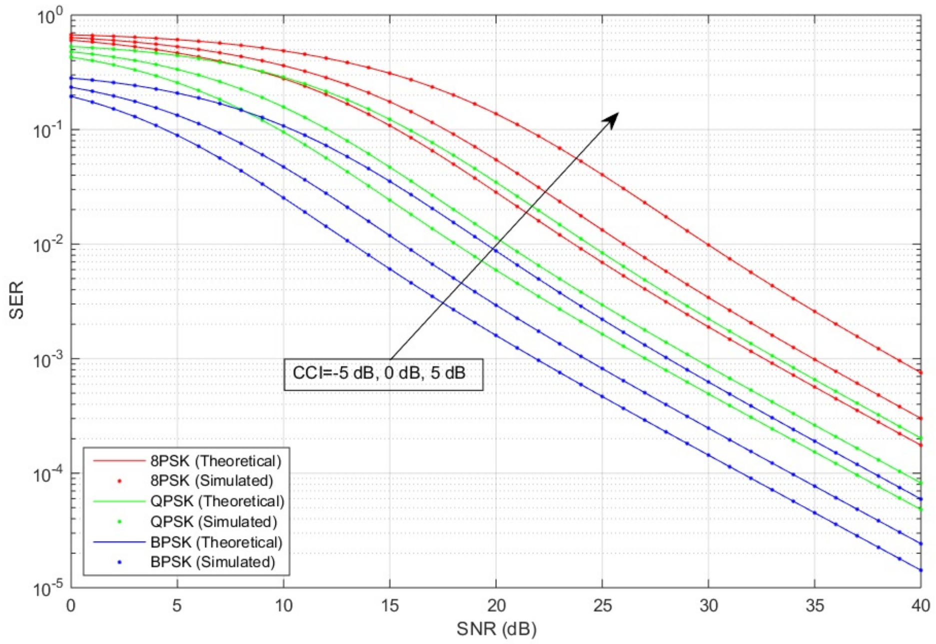

Fig. 2. Average SER versus SNR for M-PSK with CCI in average shadowing

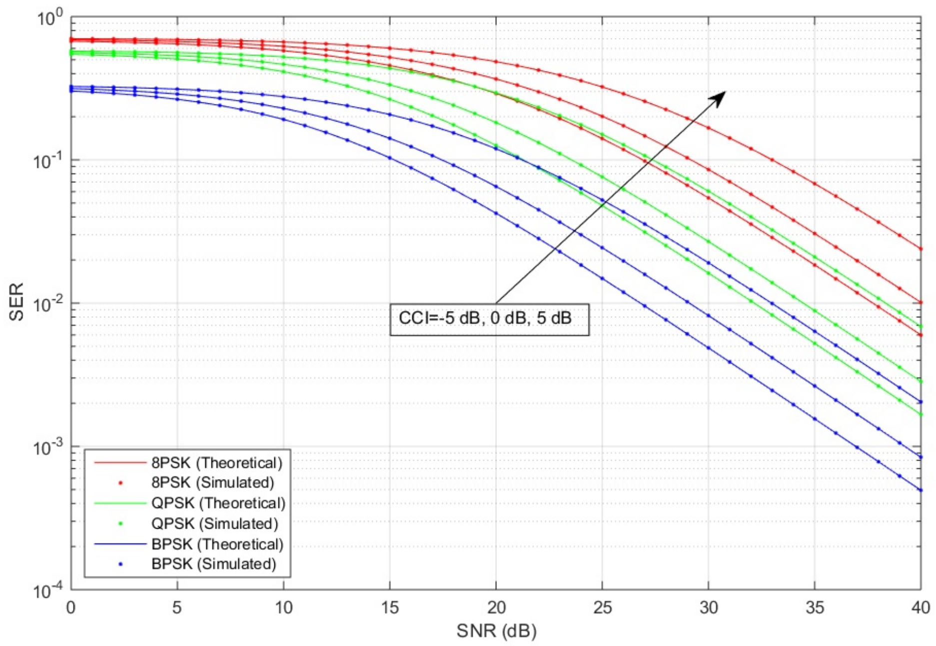

Fig. 3. Average SER versus SNR for M-PSK with CCI in frequent heavy shadowing

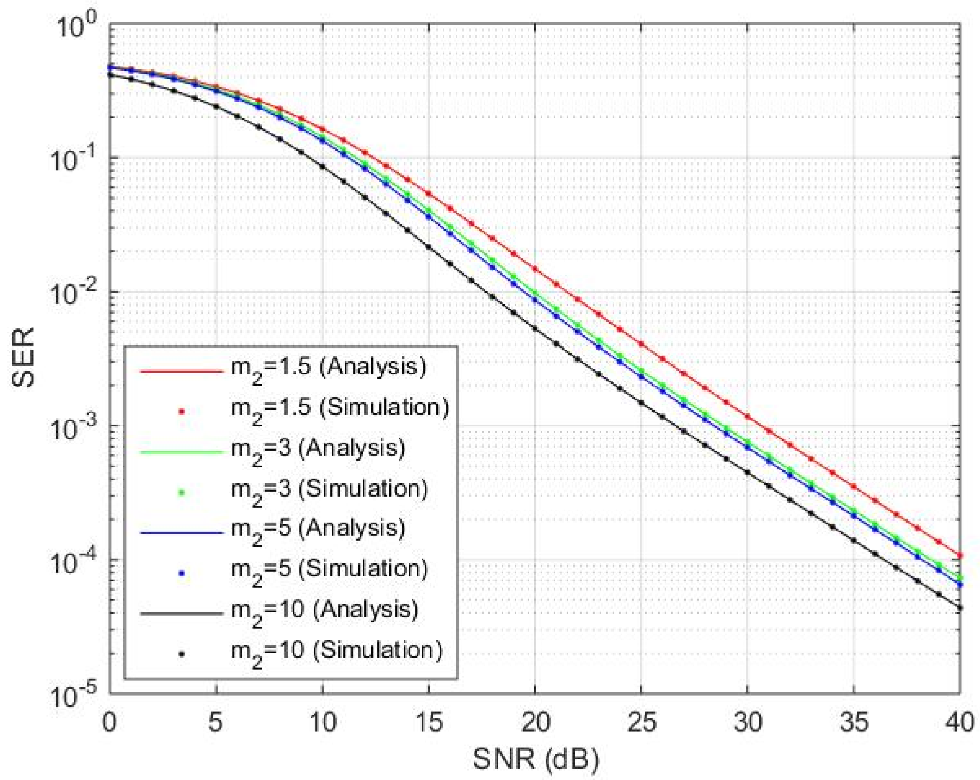

Fig. 4. Impact of the fading severity of the relay-destination link

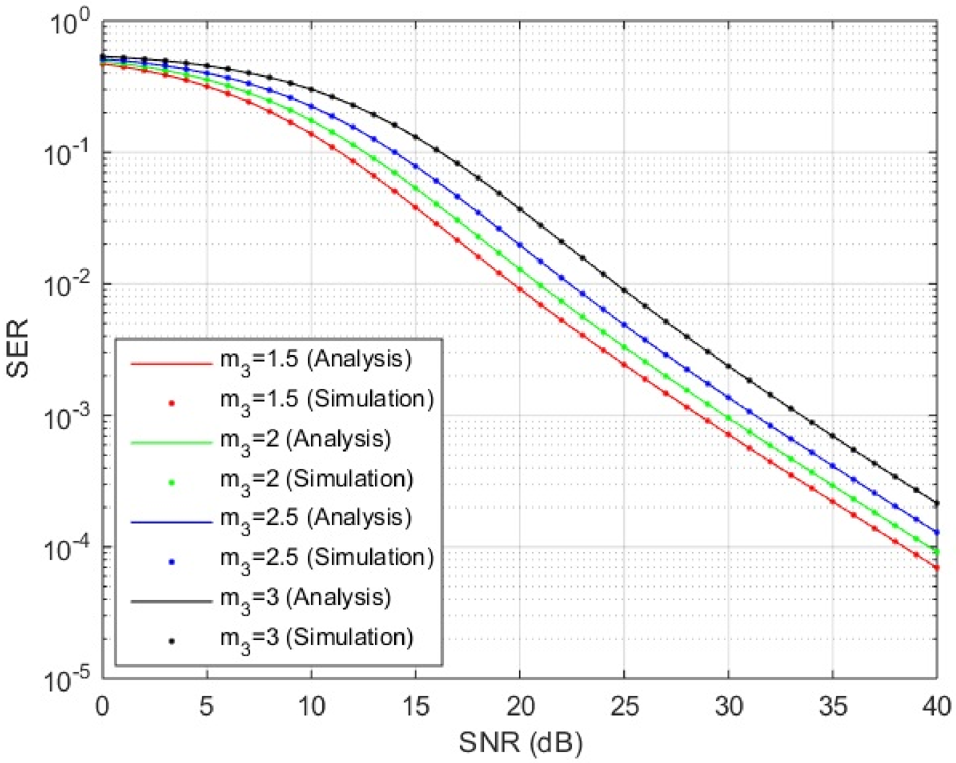

Fig. 5. Impact of the fading severity of the interferers-relay links

5. Conclusion

In this paper, we have investigated the performance of AF based hybrid satellite-terrestrial cooperative system in an interference environment. We have examined the average SER of a HSTRN with multiple interferers at the relay. We have derived the average SER of the considered system under the assumption of generalized fading channels. Our analysis has shown that CCI causes significant degradation in SER performance of AF based hybrid satellite-terrestrial cooperative system. Our results are valuable in understanding how interference at the relay can degrade the overall performance, depending on different channel, interference and network parameters.

Appendix I

On substituting (3) in (12) and after some algebraic operations, we get

$$I_1 = \alpha_1 \int_0^{\infty} e^{-\left(s\frac{y}{y\left(1+z\frac{E_i}{\sigma_1^2}\right)+C}\frac{E_s}{\sigma_1^2}+\beta_1\right)x} {}_1F_1\left(m_1;1;\delta_1 x\right)dx. \tag{31}$$

By using [25, Eq. (7.621.4)] in (31), we get

$$I_1 = \alpha_1 \left(s \frac{y}{y\left(1+z\frac{E_i}{\sigma_1^2}\right)+C} \frac{E_s}{\sigma_1^2} + \beta_1 \right)^{-1} F\left(m_1;1;1;\delta_1 \left(s \frac{y}{y\left(1+z\frac{E_i}{\sigma_1^2}\right)+C} \frac{E_s}{\sigma_1^2} + \beta_1 \right)^{-1} \right).$$

By applying [25, Eq. (9.121.1)] in above equation, one gets

$$I_1 = \frac{\alpha_1}{s \frac{y}{y\left(1+z\frac{E_i}{\sigma_1^2}\right)+C} \frac{E_s}{\sigma_1^2} + \beta_1} \left(1 - \frac{\delta_1}{s \frac{y}{y\left(1+z\frac{E_i}{\sigma_1^2}\right)+C} \frac{E_s}{\sigma_1^2} + \beta_1} \right)^{-m_1}. \tag{32}$$

From (32) we define I_{11} as follows:

$$I_{11} \triangleq \frac{\alpha_1}{s \frac{y}{y\left(1+z\frac{E_i}{\sigma_1^2}\right)+C} \frac{E_s}{\sigma_1^2} + \beta_1}. \tag{33}$$

After some modifications (33) changes to

$$I_{11} = \frac{\alpha_1 y\left(1+z\frac{E_i}{\sigma_1^2}\right) + \alpha_1 C}{\left(\left(s\frac{E_s}{\sigma_1^2} + \beta_1\left(1+z\frac{E_i}{\sigma_1^2}\right)\right) y + C\beta_1\right)}. \tag{34}$$

From (32) we define I_{12} as follows:

$$I_{12} \triangleq \left(1 - \left(\delta_1 \middle/ \left(\frac{sy}{y\left(1+z\frac{E_i}{\sigma_1^2}\right)+C} \frac{E_s}{\sigma_1^2} + \beta_1 \right) \right) \right)^{-m_1}. \tag{35}$$

After some simple steps (35) simplifies to

$$I_{12} = \frac{\left(\left(s\frac{E_s}{\sigma_1^2} + (\beta_1-\delta_1)\left(1+z\frac{E_i}{\sigma_1^2}\right)\right) y + C(\beta_1-\delta_1)\right)^{-m_1}}{\left(\left(s\frac{E_s}{\sigma_1^2} + \beta_1\left(1+z\frac{E_i}{\sigma_1^2}\right)\right) y + C\beta_1\right)^{-m_1}}. \tag{36}$$

We substitute I_{11} and I_{12} from (34) and (36), respectively in (32) to get (13) for I_1.

Appendix II

In the following we define and simplify P_1, P_2 & P_3. In the following, we extend and modify the method sketched in Appendix A of [4].

First consider P_1,

$$P_1 = \lambda_2 \sum_{l=0}^{c_1} \binom{c_1}{l} \left(s\frac{E_s}{\sigma_1^2} + \beta_1 \left(1 + z\frac{E_i}{\sigma_1^2}\right)\right)^l (C\beta_1)^{c_1-l+e} \int_0^{C\beta_1 \Big/ \left(s\frac{E_s}{\sigma_1^2} + \beta_1\left(1+z\frac{E_i}{\sigma_1^2}\right)\right)} y^{m_2+l-1} \times \frac{\left(\alpha_1\left(1+z\frac{E_i}{\sigma_1^2}\right)y + \alpha_1 C\right)\left(1 + \frac{e\left(s\frac{E_s}{\sigma_1^2} + \beta_1\left(1+z\frac{E_i}{\sigma_1^2}\right)\right)y}{C\beta_1}\right) e^{-\varepsilon_2 y}}{\left(\left(s\frac{E_s}{\sigma_1^2} + (\beta_1 - \delta_1)\left(1+z\frac{E_i}{\sigma_1^2}\right)\right)y + C(\beta_1 - \delta_1)\right)^{m_1}} dy. \tag{37}$$

To simplify (37), we do the following substitution of variable: $y = C\beta_1 x \Big/ \left(\left(sE_s \big/ \sigma_1^2\right) + \beta_1\left(1 + zE_i \big/ \sigma_1^2\right)\right)$, and finally get (19).

Now consider P_2,

$$P_2 = \lambda_2 \sum_{l=0}^{c_1} \binom{c_1}{l} \left(s\frac{E_s}{\sigma_1^2} + \beta_1 \left(1 + z\frac{E_i}{\sigma_1^2}\right)\right)^{l+e} (C\beta_1)^{c_1-l} \int_0^{C\beta_1 \Big/ \left(s\frac{E_s}{\sigma_1^2} + \beta_1\left(1+z\frac{E_i}{\sigma_1^2}\right)\right)} y^{m_2+l+e-1} \times \frac{\left(\alpha_1\left(1+z\frac{E_i}{\sigma_1^2}\right)y + \alpha_1 C\right)\left(1 + \frac{eC\beta_1}{\left(s\frac{E_s}{\sigma_1^2} + \beta_1\left(1+z\frac{E_i}{\sigma_1^2}\right)\right)y}\right) e^{-\varepsilon_2 y}}{\left(\left(s\frac{E_s}{\sigma_1^2} + (\beta_1 - \delta_1)\left(1+z\frac{E_i}{\sigma_1^2}\right)\right)y + C(\beta_1 - \delta_1)\right)^{m_1}} dy. \tag{38}$$

To simplify (38), we do the following substitution of variable: $y = C\beta_1 x \Big/ \left(sE_s \big/ \sigma_1^2 + \beta_1\left(1 + zE_i \big/ \sigma_1^2\right)\right)$, and finally get (20).

Finally consider P_3,

$$P_3 = \lambda_2 \sum_{l=0}^{c_1} \binom{c_1}{l} \left(s\frac{E_s}{\sigma_1^2} + \beta_1 \left(1 + z\frac{E_i}{\sigma_1^2}\right)\right)^{l+e} (C\beta_1)^{c_1-l} \int_0^{\infty} y^{m_2+l+e-1} \times \frac{\left(\alpha_1\left(1+z\frac{E_i}{\sigma_1^2}\right)y + \alpha_1 C\right)\left(1 + \frac{eC\beta_1}{\left(s\frac{E_s}{\sigma_1^2} + \beta_1\left(1+z\frac{E_i}{\sigma_1^2}\right)\right)y}\right) e^{-\varepsilon_2 y}}{\left(\left(s\frac{E_s}{\sigma_1^2} + (\beta_1 - \delta_1)\left(1+z\frac{E_i}{\sigma_1^2}\right)\right)y + C(\beta_1 - \delta_1)\right)^{m_1}} dy. \tag{39}$$

We introduce the following function:

$$f(a) \triangleq \frac{\Gamma(a+1)C^{a+1-m_1}(\beta_1-\delta_1)^{a+1-m_1}}{\left(s\frac{E_s}{\sigma_1^2}+(\beta_1-\delta_1)\left(1+z\frac{E_i}{\sigma_1^2}\right)\right)^{a+1}} \times \psi\left(a+1, a+2-m_1; \frac{\varepsilon_2 C(\beta_1-\delta_1)}{s\frac{E_s}{\sigma_1^2}+(\beta_1-\delta_1)\left(1+z\frac{E_i}{\sigma_1^2}\right)}\right), \tag{40}$$

where $\psi(\alpha,\gamma;z)$ is defined in [25, Eq. (9.210.2)].

By using integral representation [25, Eq. (9.211.4)] of $\psi(\alpha,\gamma;z)$, (40) becomes

$$f(a) \triangleq \frac{\Gamma(a+1)C^{a+1-m_1}(\beta_1-\delta_1)^{a+1-m_1}}{\left(s\frac{E_s}{\sigma_1^2}+(\beta_1-\delta_1)\left(1+z\frac{E_i}{\sigma_1^2}\right)\right)^{a+1}} \times \frac{1}{\Gamma(a+1)}\int_0^\infty e^{-\frac{\varepsilon_2 C(\beta_1-\delta_1)}{s\frac{E_s}{\sigma_1^2}+(\beta_1-\delta_1)\left(1+z\frac{E_i}{\sigma_1^2}\right)}t} t^a (1+t)^{-m_1}\, dt. \tag{41}$$

The integral in (39) is solved by first using [30, Eq. (2.3.6.9)], and then making use of (41) to express the result succinctly. Doing so leads us finally to (21).

References

[1] Barry Evans, Markus Werner, Erich Lutz, Michel Bousquet, Giovanni E. Corazza, Gerard Maral, Robert Rumeau and Erina Ferro, "Integration of satellite and terrestrial systems in future multimedia communications," *IEEE Wireless Communications*, vol. 12, no. 5, pp. 72-80, October, 2005. Article (CrossRef Link)

[2] Vasileios K. Sakarellos, Charilaos Kourogiorgas and Athanasios D. Panagopoulos, "Cooperative Hybrid Land Mobile Satellite-Terrestrial Broadcasting Systems: Outage Probability Evaluation and Accurate Simulation," *Wireless Personal Communication*, vol. 79, no. 2, pp. 1471-1481, November, 2014. Article (CrossRef Link)

[3] Arif Iqbal and Kazi M Ahmed, "A Hybrid Satellite-Terrestrial Cooperative Network over Non Identically Distributed Fading Channels," *Journal of Communications*, vol. 6, no. 7, pp. 581-589, October, 2011. Article (CrossRef Link)

[4] Manav R. Bhatnagar and Arti M.K., "Performance Analysis of AF Based Hybrid Satellite-Terrestrial Cooperative Network over Generalized Fading Channels," *IEEE Communications Letters*, vol. 17, no. 10, pp. 1912-1915, October, 2013. Article (CrossRef Link)

[5] Ali Abdi, Wing C. Lau, Mohamed-Slim Alouini and Mostafa Kaveh, "A New Simple Model for Land Mobile Satellite Channels: First- and Second-Order Statistics," *IEEE Transactions on Wireless Communications*, vol. 2, no. 3, pp. 519-528, May, 2003. Article (CrossRef Link)

[6] Simone Morosi, Sara Jayousi and Enrico Del Re, "Cooperative Delay Diversity in Hybrid Satellite/Terrestrial DVB-SH System," in *Proc. of IEEE Conf. on Communications*, pp. 1-5, May 23-27, 2010. Article (CrossRef Link)

[7] Do Seob Ahn, Sooyoung Kim, Hee Wook Kim and Dong-Chul Park, "A cooperative transmit diversity scheme for mobile satellite broadcasting systems," *International Journal of Satellite Communications and Networking*, vol. 28, no. 5-6, pp. 352-368, September-December, 2010. Article (CrossRef Link)

[8] G. Cocco, C. Ibars and O. del Rio Herrero, "Cooperative satellite to land mobile gap-filler-less interactive system architecture," in *Proc. of 5th Advanced satellite multimedia systems conference (asma) and the 11th signal processing for space communications workshop (spsc)*, pp. 309-314, September 13-15, 2010. Article (CrossRef Link)

[9] Beatrice Paillassa, Benoit Escrig, Riadh Dhaou, Marie-Laure Boucheret and Caroline Bes, "A cooperative transmit diversity scheme for mobile satellite broadcasting systems," *International Journal of Satellite Communications and Networking*, vol. 29, no. 6, pp. 479-500, November-December, 2011. Article (CrossRef Link)

[10] Vasileios. K. Sakarellos and Athanasios. D. Panagopoulos, "Outage performance of cooperative Land Mobile Satellite broadcasting systems," in *Proc. of 7th European Conference on Antennas and Propagation (EuCAP)*, pp. 473-476, April 8-12, 2013. Article (CrossRef Link)

[11] Sokchenda Sreng, Benoit Escrig and Marie-Laure Boucheret, "Exact Outage Probability of a Hybrid Satellite Terrestrial Cooperative System with Best Relay Selection," in *Proc. of IEEE Conf. on Communications*, pp. 4520-4524, June 9-13, 2013. Article (CrossRef Link)

[12] Sokchenda Sreng, Benoit Escrig and Marie-Laure Boucheret, "Exact Symbol Error Probability of Hybrid/Integrated Satellite-Terrestrial Cooperative Network," *IEEE Transactions on Wireless Communications*, vol. 12, no. 3, pp. 1310-1319, March, 2013. Article (CrossRef Link)

[13] Manav R. Bhatnagar and Arti M.K., "Performance Analysis of Hybrid Satellite-Terrestrial FSO Cooperative System," *IEEE Photonics Technology Letters*, vol. 25, no. 22, pp. 2197-2200, November, 2013. Article (CrossRef Link)

[14] Arti M.K. and Manav R. Bhatnagar, "Beamforming and Combining in Hybrid Satellite-Terrestrial Cooperative Systems," *IEEE Communication Letters*, vol. 18, no. 3, pp. 483-486, March, 2014. Article (CrossRef Link)

[15] Manav R. Bhatnagar and Arti M.K., "On the Closed-Form Performance Analysis of Maximal Ratio Combining in Shadowed-Rician Fading LMS Channels," *IEEE Communications Letters*, vol. 18, no. 1, pp. 54-57, January, 2014. Article (CrossRef Link)

[16] Manav R. Bhatnagar, "On the Sum of Correlated Squared $\kappa-\mu$ Shadowed Random Variables and its Application to Performance Analysis of MRC," *IEEE Transactions on Vehicular Technology*, vol. 64, no. 6, pp. 2678-2684, June, 2015. Article (CrossRef Link)

[17] Caijun Zhong, Shi Jin and Kai-Kit Wong, "Dual-hop systems with noisy relay and interference-limited destination," *IEEE Transactions on Communications*, vol. 58, no. 3, pp. 764-768, March, 2010. Article (CrossRef Link)

[18] Kang An, Min Lin, Jian Ouyang and Heng Wei, "Beamforming in Dual-Hop AF Relaying with Imperfect CSI and Co-channel Interference," *Wireless Personal Communication*, vol. 78, no. 2, pp. 1187-1197, September, 2014. Article (CrossRef Link)

[19] Yuzhen Huang, Fawaz Al-Qahtani, Caijun Zhong, Qihui Wu, Jinlong Wang and Hussein Alnuweiri, "Performance Analysis of Multiuser Multiple Antenna Relaying Networks with Co-Channel Interference and Feedback Delay," *IEEE Transactions on Communications*, vol. 62, no. 1, pp. 59-73, January, 2014. Article (CrossRef Link)

[20] Jinlong Wang, Yuzhen Huang, Caijun Zhong, Fawaz Al-Qahtani, Qihui Wu, and Yunpeng Cheng, "Performance analysis of interference-limited dual-hop multiple antenna AF relaying systems with feedback delay," EURASIP Journal on Wireless Communications and Networking 2013 2013:284. Article (CrossRef Link)

[21] Kang An, Min Lin, Jian Ouyang, Yongming Huang and Gan Zheng, "Symbol Error Analysis of Hybrid Satellite-Terrestrial Cooperative Networks With Cochannel Interference," *IEEE Communications Letters*, vol. 18, no. 11, pp. 1947-1950, November, 2014. Article (CrossRef Link)

[22] Daniel Benevides da Costa, Haiyang Ding and Jianhua Ge, "Interference-Limited Relaying Transmissions in Dual-Hop Cooperative Networks over Nakagami-m Fading," *IEEE Communications Letters*, vol. 15, no. 5, pp. 54-57, May, 2011. Article (CrossRef Link)

[23] Mischa Dohler, Athanasios Gkelias and Hamid Aghvami, "Resource Allocation for FDMA-Based Regenerative Multihop Links," *IEEE Transactions on Wireless Communications*, vol. 3, no. 6, pp. 1989-1993, November, 2004. Article (CrossRef Link)

[24] Ioannis Krikidis, John S. Thompson, Steve McLaughlin and Norbert Goertz, "Max-Min Relay Selection for Legacy Amplify-and-Forward Systems with Interference," *IEEE Transactions on Wireless Communications*, vol. 8, no. 6, pp. 3016-3027, June, 2009. Article (CrossRef Link)

[25] I.S. Gradshteyn and I.M. Ryzhik, Table of Integrals, Series, and Products, 7th Edition, Elsevier/Academic Press, Amsterdam, 2007.

[26] Marvin K. Simon and Mohamed-Slim Alouini, Digital Communication over Fading Channels, 2nd Edition, Wiley, New York, 2005. Article (CrossRef Link)

[27] Himal A. Suraweera, Diomidis S. Michalopoulos and Chau Yuen, "Performance Analysis of Fixed Gain Relay Systems With a Single Interferer in Nakagami-*m* Fading Channels," *IEEE Transactions on Vehicular Technology*, vol. 61, no. 3, pp. 1457-1463, March, 2012. Article (CrossRef Link)

[28] Himal A. Suraweera, Hari K. Garg and A. Nallanathan, "Performance Analysis of Two Hop Amplify-and-Forward Systems with Interference at the Relay," *IEEE Communications Letters*, vol. 14, no. 8, pp. 692-694, January, 2010. Article (CrossRef Link)

[29] Matthew R. McKay, Alberto Zanella, Iain B. Collings and Marco Chiani, "Error Probability and SINR Analysis of Optimum Combining in Rician Fading," *IEEE Transactions on Communications*, vol. 57, no. 3, pp. 676-687, March, 2009. Article (CrossRef Link)

[30] A. P. Prudnikov, Yu. A. Brychkov and O. I. Marichev, Integrals And Series Volume 1: Elementary Functions, Gordon and Breach Science Publishers, New York, 1986.

Umer Javed received the B.S. degree in electrical engineering from University of Engineering & Technology Taxila, Taxila, Pakistan, in 2006, and the M.S. degree in communications engineering from Helsinki University of Technology, Espoo, Finland, in 2009. He is currently studying for the Ph.D. degree at Shanghai Jiao Tong University, Shanghai, China.

Di He, received the Ph.D. degree in circuits and systems from Shanghai Jiao Tong University, Shanghai, China, in 2002. From 2002 to 2004, he was with the Department of Electrical and Computer Engineering, University of Calgary, Calgary, AB, Canada, as a Postdoctoral Fellow. He is currently an Associate Professor with the School of Electronic, Information and Electrical Engineering, Shanghai Jiao Tong University. His research interests are in the areas of wireless communications, nonlinear dynamics and its applications in wireless communications and positioning.

Peilin Liu, received the D.Eng. degree from the University of Tokyo, Tokyo, Japan, in 1998. In 1999, she was a Researcher with the University of Tokyo. From 1999 to 2003, she was a Senior Researcher with the Central Research Institute of Fujitsu, Tokyo. In 2003, she joined Shanghai Jiao Tong University, Shanghai, China, where she is currently a Professor with the Department of Electronic Engineering. She also directs the MediaSoC Lab and codirects the Shanghai Key Laboratory of Navigation and Location-based Services.